Engineering Structures 30 (2008) 3074–3081

Contents lists available at ScienceDirect

Engineering Structures

journal homepage: www.elsevier.com/locate/engstruct

Settlement analysis of the Mornos earth dam (Greece): Evidence from numerical modeling and geodetic monitoring

Vassilis Gikas [a,*], Michael Sakellariou [b]

[a] Laboratory of General Geodesy, School of Rural and Surveying Engineering, National Technical University of Athens, GR 15780, Greece

[b] Laboratory of Structural Mechanics and Technical Works, School of Rural and Surveying Engineering, National Technical University of Athens, GR 15780, Greece

ARTICLE INFO

Article history:
Received 28 December 2007
Received in revised form
28 March 2008
Accepted 31 March 2008
Available online 27 May 2008

Keywords:
Dam settlement
Finite element analysis
Precise leveling
Deformation monitoring of structures

ABSTRACT

This paper studies the long-term (>30 years) settlement behavior of the Mornos dam on the basis of finite element analysis and vertical displacement data. It compares actually measured deformations resulting from a continuous geodetic monitoring record of the dam behavior with a numerical back analysis. Our aim is to explain the actual deformation history on the basis of the mechanical behavior of the dam. The deformation monitoring record consists of precise leveling data of a large number of control stations established along the crest and the inspection gallery of the dam, as well as settlements derived by magnetic extensometers placed inside the dam body. Overall, the available data cover the phases of construction, first filling of the reservoir and most of the operational time of the dam. The numerical modeling assumes 2D plane-strain conditions to obtain the displacement and the stress–strain characteristics of the abutments and the dam at eleven equally-spaced cross sections. Comparative evaluation of the results of the geodetic monitoring analysis against the findings from the finite element back analysis simulating characteristic stages in the lifetime of the structure, shows a very good agreement (on average 0.03 m) between the measured and computed displacements, which testifies to the correctness of the geotechnical parameters and loads used in the analysis.

1. Introduction

The safety of large man-made structures, the environmental protection and the development of associated mitigating measures in the case of natural disasters, require a good understanding of the causes and the mechanism of the structural deformation process. In the case of earthen dams, the most well-known causes of failure relate to construction defects that induce erosion and/or excessive pore pressures/hydraulic gradients to the embankments, under the foundation or the abutments of the structure that result in stability problems in the dam body [1,2]. Other less common causes of damage are high water pressures and liquefaction due to ground motion caused by earthquakes [3].

At the design stage of a dam, a relationship can be established between the causative factors (loads) and the expected deformation (displacement and strain), using various numerical methods [4]. In this context, the finite-element method (FEM) is widely accepted nowadays for its ability to model complex geometries, peculiar geological conditions and a variety of boundary conditions [5–7]. The results of such analyses coupled with the analyses of field measurements (topographical, geotechnical, hydrological, etc.) lead to decision-making regarding the construction parameters (geometry, material, method of material placement and compaction, etc.) of a dam project. Likewise, during all phases (construction, first filling of the reservoir and operation) in the lifetime of a dam, deformation monitoring provides base data for a geometrical analysis in the space and time domains [8–10]. Comparative evaluation of these analyses against the findings of numerical modeling is essential for the safety of the structure, as well as for regular maintenance operations. Furthermore, it is evident that detailed studies based on such comparisons are useful for gaining experience for future designs. Nevertheless, despite the fact that exhaustive deformation monitoring is nowadays a prerequisite for most dam projects worldwide, the published results of the comparisons derived between predicted (e.g. from FEM) and observed deformations are usually limited to the stages of construction and the first filling of the reservoir [3,11]. Comparative results that cover long periods of the lifetime of a dam are rare in the literature (e.g. [12]) due to unreliable or incomplete data records.

This paper compares actually measured deformations resulting from a continuous geodetic monitoring record of Mornos dam behavior with a numerical back analysis. Our aim is to explain the actual deformation history on the basis of the mechanical behavior of the dam. Analysis focuses on vertical displacements while the available geodetic data span a total period of 30 years

* Corresponding author. Tel.: +30 210 772 3566; fax: +30 210 772 2728.
E-mail addresses: vgikas@central.ntua.gr (V. Gikas), mgsakel@mail.ntua.gr (M. Sakellariou).

0141-0296/$ – see front matter © 2008 Elsevier Ltd. All rights reserved.
doi:10.1016/j.engstruct.2008.03.019

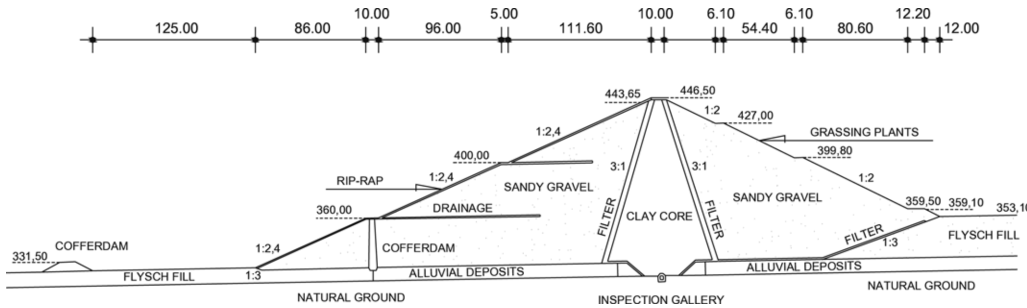

Fig. 1. Typical cross section of Mornos dam.

Table 1
Technical characteristics of Mornos dam and reservoir

Dam detail	Value
Height of crest	126 m
Dam crest elevation a.s.l.	+ 446.5 m
Length of dam crest	815 m
Width of dam crest	10 m
Dam slope upstream	1:2.4 + berms
Dam slope downstream	1:2.0 + berms
Total dam volume	17×10^6 m^3
Total reservoir area	18.5 km^2
Total reservoir volume	780×10^6 m^3
Usable reservoir volume	640×10^6 m^3

of measurements, which covers part of the construction phase, the stage of first filling of the reservoir and most of its operational lifetime. Additionally, some comparisons based on magnetic extensometer measurements are performed. The processing technique adopted in this study for numerical modeling relies on the FEM approach, realized in two-dimensional plain-strain conditions.

2. Main features of the Mornos dam

The Mornos dam is the largest in a sequence of water works which began in the 1920s in order to secure water supplies for the capital of Greece, Athens. It is located in the upper route of the Mornos river near the small town of Lidoriki and approximately 220 km W-NW of Athens. The construction of the dam began in 1973 and completed in early 1977, while the filling of the reservoir was carried out in several sequential steps over the period 1979–1981. The technical characteristics of the dam and the reservoir are given in Table 1.

From a geological viewpoint, the dam site and most of the reservoir area are situated on formations of impervious flysch and fine to medium grained sandstone. However, on the right abutment of the dam and in certain areas of the reservoir, the flysch is pervious to depths of dozens of meters. In these areas water tightening was undertaken by means of a grouting curtain, reaching a maximum depth of 95 m [13]. In contrast, the left abutment consists mainly of solid sandstone. The dam section is composed of a central clay core, transition zones and sand-gravel pervious shells (Fig. 1). The upstream slope is lined with protective rip-rap, while the downstream slope is covered with grass and shrubs. The main cofferdam is incorporated in the dam section, which is provided with a central impervious core and a foundation cut-off diaphragm.

3. The deformation monitoring system

The technical characteristics of the dam in combination with the intensely disordered geological formations of the wider area have led to the adoption of a detailed monitoring program that encompasses a variety of geotechnical and geodetic instruments and techniques. The field instrumentation placed in the dam body includes a total of 12 magnetic extensometer systems, 34 earth pressure cells, 54 piezometers at various depths, and 2 accelerometers at the crest and the foundation layers of the dam respectively, to record the seismic activity [13]. In addition to geotechnical monitoring, periodic geodetic surveys have been undertaken since the construction stages of the dam. The geodetic monitoring system consists of 15 reference stations that spread over an area as far as 2.5 km from the dam site and 53 control stations established at the crest, the abutments and the downstream shell of the dam [14,15]. The surveys employ conventional geodetic instruments and techniques, whereas in more recent years (2002–2004), satellite (GPS) survey methods were implemented [16]. Furthermore, due to the paramount significance of the project, and its location within the earthquake prone area of the Gulf of Corinth, extensive GPS campaigns were undertaken in the greater area of the reservoir between 1993 and 2003 in order to study its crystal behavior. From these studies, it can be concluded that the area surrounding the reservoir exhibits similar tectonic behavior and follows the general trends observed in Central Greece from independent research work [17,18].

4. Settlement monitoring and analysis

Since the Mornos dam is a large embankment structure, its fill material and the foundation is subject to significant vertical displacements. As expected, deformation developed fast during the construction phase and the stage of the first filling of the reservoir, and decreased progressively in time. The monitoring system of vertical displacements relies on precise leveling observations and measurements of magnetic extensometers. Table 2 presents the time span of all available data.

4.1. Precise leveling measurements

Precise geometric leveling measurements are taken from the control stations established at the crest of the dam and from the control stations set out on the level sections at the inspection gallery (Figs. 2 and 3). The grouting gallery is located along the dam axis, 135 m below the crest and below the core base, branching into horizontal tunnels on the abutments. The vertical displacements of these stations were measured using a high accuracy spirit level (a Zeiss Ni2 initially and a Leica NA2 more recently), relative to a fixed benchmark established on solid ground. At the sloping sections of the gallery, the method of trigonometric leveling was applied, using initially a Wild Distomat DI 3S in combination with a Wild T2, and in the more recent campaigns a Leica TC 1600. The geodetic leveling network incorporates a total of 17 control stations on the crest and 15 primary control stations in the inspection gallery. The accuracy of the vertical displacements was estimated better than 1.7 mm/km for the geometric leveling and 3.6 mm/km for the trigonometric leveling [19]. As depicted in Table 2, the available time series for the control points on the crest of the dam cover most of the post-construction period up to the present day. In contrast, the available data for the control stations in the dam gallery are restricted to a limited number of surveys, spanning the entire lifetime of the dam.

Fig. 4 shows the progression of the vertical displacements of control station S20 located at the middle of the crest at height 135 m, and of control station S28 located towards the tail-end of the crest at height 110 m for a total period of 26 years, i.e. it covers the stages of post-construction and first filling of the reservoir and most of its operational lifetime. From this graph two points are immediately evident: firstly, the displacements cumulate over time but they are approaching to their final values; secondly, the settlement at the middle of the dam is much larger compared to the settlement observed near the tail-ends of the crest (0.47 m vs. 0.31 m). The difference in height between the two stations explains the observed difference of settlements. The trend of the curves indicates a typical consolidation behavior, which is approximated by a 4th degree polynomial. Fig. 5 provides a more comprehensive representation of the crest settlement. It summarizes the vertical displacements for all stations on the dam crest. From this graph it is evident that the maximum displacement is at the middle of the crest. Also, it is important to note that 60% of the total displacement for the period between 1977 and 2006 occurred during the post-construction and first filling stages of the lake, while the remaining 40% developed during the operation (and significantly longer) period of the dam's life, which also suggests that the dam tends to stabilize.

The displacements observed at the gallery of the dam exhibit a similar trend to the displacements observed at the crest. However, as expected they are significantly smaller. Fig. 6 contains the

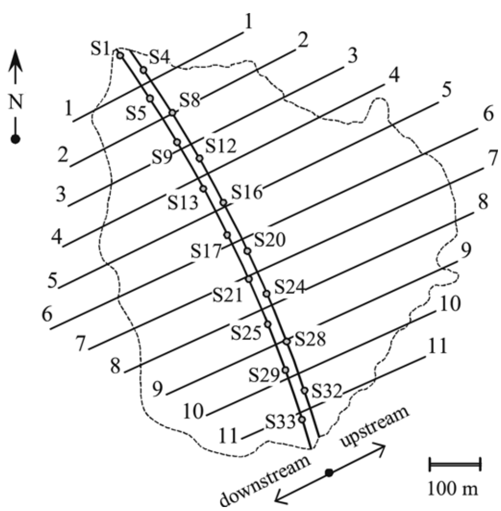

Fig. 2. Location of the control stations established at the crest of the dam and distribution of the cross sections adopted in the FEM analysis.

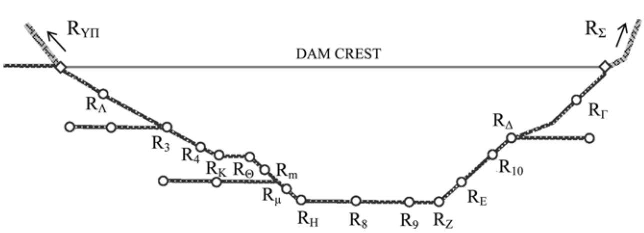

Fig. 3. Upstream face of the dam showing the inspection gallery branching into horizontal tunnels on the abutments.

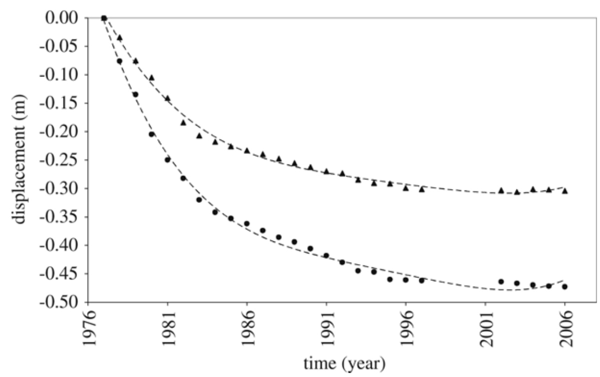

Fig. 4. Time series of vertical displacements observed by precise leveling at control stations S20 located at the middle of the crest (circles), and S28 located towards the tail-end of the crest (triangles).

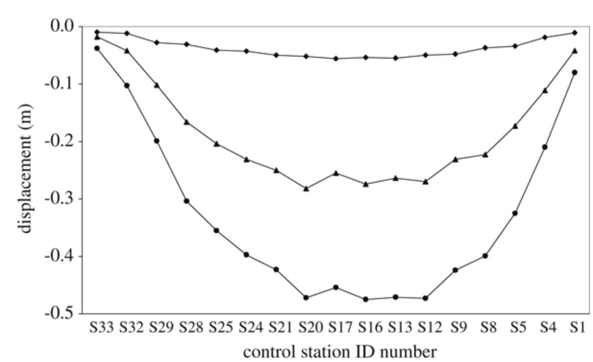

Fig. 5. Developed view of the vertical displacements estimated by precise leveling at the crest of the dam. The three lines correspond to the displacements for the period after the completion of construction in 1978 (rhombs), at the completion of first filling of the reservoir in 1982 (triangles), and for year 2006 (circles).

Table 2
Temporal distribution of available settlement data

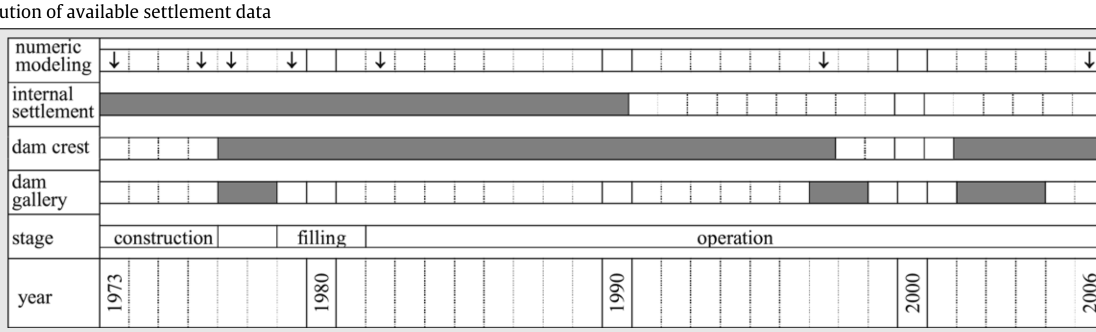

The arrows indicate the years for which FEM analyses were computed.

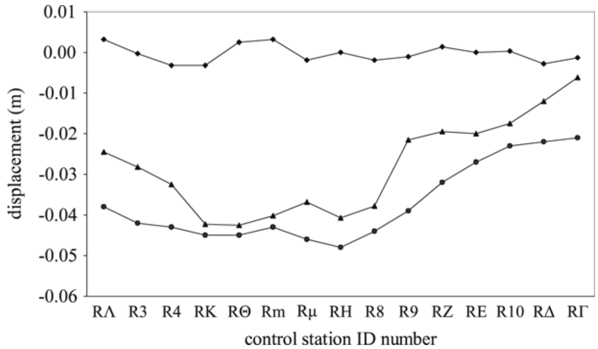

Fig. 6. Developed view of the vertical displacements observed by precise leveling at the gallery of the dam. The three lines correspond to the displacements observed for the time periods: 1977–1978 (rhombs), 1977–1998 (triangles) and 1977–2004 (circles).

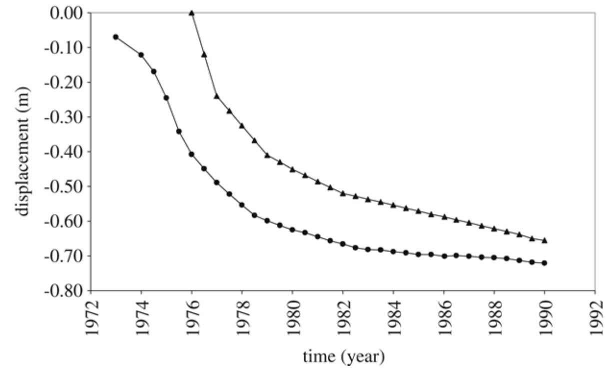

Fig. 7. Internal settlements recorded at the central cross section, at the lower (circles) and the top (triangles) layers of the dam for the period 1973–1990 and 1976–1990 respectively.

vertical displacements for the periods 1977–1978, 1977–1998 and 1977–2004. A close examination of this graph reveals that in the first 21 years (1977–1998), the maximum displacement occurred at the middle of the dam and reached 0.042 m. It is interesting to note that the vertical displacements which occurred on the right side of the dam are considerably smaller than those on the left side of the dam. In the period 1997–2004 the maximum displacement does not exceed 0.015 m. Overall, these results indicate that the magnitude of the vertical movements is seen to decrease with time, adding further confirmation that the dam tends to stabilize.

4.2. Internal settlement measurements

The vertical displacements inside the dam body were measured using magnetic probe extensometers. These are distributed in four cross sections. More specifically, three extensometer systems were placed in every section; one in the center of the dam and two in the upstream and downstream shells, respectively. Their accuracy is dependent on the visual readout of the markings on the survey tape used and magnetic probes are difficult to fix in case of malfunction. Nevertheless, they are very useful because they provide measures of settlement within the dam body. Also, the measurements cover the period of the construction of the dam for which no geodetic data exist.

Fig. 7 shows the progression of the vertical displacements observed at the lower and the top layers (95 m and 3 m below the crest respectively), in the middle of the dam (cross section 6-6) for the periods 1973–1990 and 1976–1990. From this plot it is evident that the maximum settlement occurs during the time of construction, decreasing steadily until 1990, when the settlement sensors were disabled.

5. Finite element model construction

The FEM elasto-plastic analyses were performed using the structural analysis software *Z_Soil* ®, developed by *Zace Ltd* in collaboration with a number of academic institutes [20]. In *Z_Soil* ®, a model of the dam site area was constructed in order to study the geometric changes and the stress–strain behavior of the dam. In essence, three basic models have been analyzed, which relate to the periods during the staged construction of the dam, the gradual filling of the reservoir, and the operating period of the dam [21,22].

5.1. Geometry model

In this study, the numerical modeling is performed under plane-strain conditions. More specifically, a total of eleven equally-spaced cross sections were taken into consideration as shown in Fig. 2. The FEM model for the upstream and downstream embankments extends 300 m in both directions, whereas the depth of the model is twice the maximum height of the dam (252 m). The FEM mesh for every plane modeled consists of approximately 4000 nodes. Fig. 8 shows a detail of the analyzed cross section in the middle of the dam. Finally, a particularly fine FEM mesh was built around the grouting gallery in view of the high stress gradients in this area (Fig. 9).

5.2. Geotechnical parameters of the materials

Some rudimentary information concerning the material parameters used in the analyses were taken from Tsatsanifos [23]. Table 3 lists the material properties finally accepted for the analysis. In Table 3, E is the elastic modulus, v is the Poisson ratio, γ is the specific weight, c is the cohesion and φ the angle of friction. It is noted that, there is not available a FE analysis of the dam from its design; only a stability analysis was performed based on Sarma's

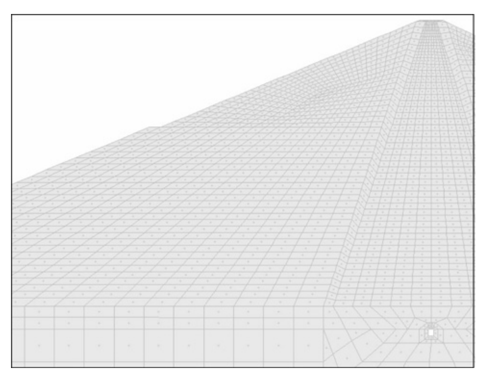

Fig. 8. Detail of the FEM mesh of the central cross section 6-6.

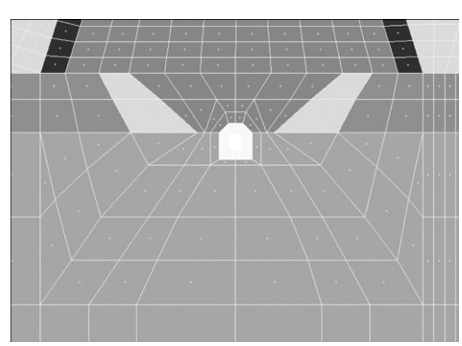

Fig. 9. FEM mesh around the inspection gallery.

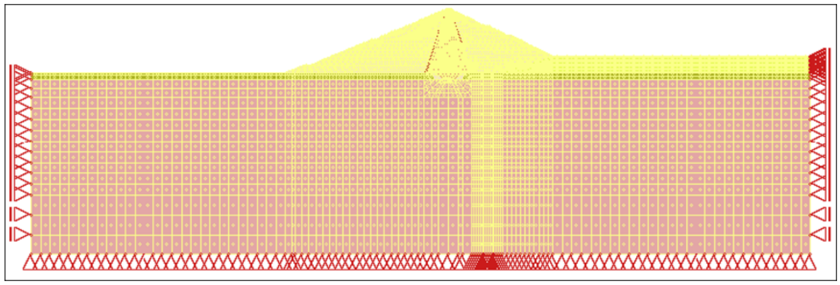

Fig. 10. Boundary conditions applied in the FEM analysis at the sides and the bottom of each cross section.

Table 3
List of material properties used in FEM analyses

Material type	Material properties						
	E (kN/m^2)	v	γ_{dry} (kN/m^3)	γ_w (kN/m^3)	c (kN/m^2)	φ (deg)	k (m/s)
Foundation rock layer	500×10^3	0.2	20	10	–	–	–
Clay core	75×10^3	0.3	18.5	10	24	26	10^{-7}
Sand gravel shell	150×10^3	0.3	22	10	1	40	10^{-5}
Sand gravel alluvial	100×10^3	0.3	19	10	1	37	10^{-5}
Gravel drainage	200×10^3	0.3	20	10	–	–	10^{-3}
Weathered flysch	100×10^3	0.3	20	10	1	40	10^{-5}
Concrete in gallery	200×10^3	0.2	24	10	–	–	–

method [23]. Therefore, for the purpose of this work reasonable values for the elastic modulus of the materials were assumed so that, the total settlement of the dam should not exceed 1% of its height [1], and the clay core was well compacted during the construction [24]. Also, in the analysis, the Drucker–Prager failure criterion was used as it results in a smooth failure envelope and is applicable for clay type and rock materials [25].

5.3. Geotechnical modeling

The FEM analysis takes into consideration the combination of three types of loads; gravity load, water pressure and seepage forces. The gravity load was applied by assigning the unit weight of the materials. For the models associated with the stages of first filling of the reservoir and the operating time of the dam, static water pressure was applied as a surface load on the upstream embankment.

As for the boundary conditions, the vertical displacements were restrained at the sides and the bottom of each cross section, by applying the "box shaped" solid boundary shown in Fig. 10. In addition, for the models for which deformation was coupled with flow, hydraulic conditions were applied on the fluid and seepage head of the dam. Table 4 shows the stages of analysis, the corresponding type of analysis and the drivers used in *Z_Soil* ®software [20].

Table 4
Stages, type of analysis and drivers used in *Z_Soil* ®software in geotechnical modeling

Stage	Type of analysis	Analysis drivers
Incremental construction of dam	Deformation	Initial state Time dependent *(Driven load)* Stability ($c - \varphi$)
End of construction	Deformation	Time dependent *(Driven load)* Stability ($c - \varphi$)
Fill of dam's lake	Deformation + Flow	Time dependent *(Driven load)* Stability ($c - \varphi$)
Stage of operation	Deformation + Flow	Time dependent *(Driven load)* Stability ($c - \varphi$)
Flow through the dam during operation	Flow	Initial state Time dependent *(Transient)*

6. Results of numerical modeling

For the three basic models adopted in the previous section, the finite-element analysis produced detailed measures of the stress–strain and the deformation distribution of the dam body. It is noted that, in order to account for the effect of gradual increase in the self weight of the dam during the construction on its mechanical behaviour, the numerical modeling for the period 1973–1976 was performed in stages to reflect the progress in the construction program. After several iterative analyses, a model that consists of twenty sequential stages was adopted.

The results depicted in Figs. 11 and 12 form typical examples of the analyses. Fig. 11 shows the FEM calculated profile of the total vertical displacement computed at the middle of the dam (cross section 6–6) for the period 1973–1982. This graph reveals a generally symmetric distribution of settlements, with respect to the vertical passing through the dam axis. The maximum values refer to the crest of the dam. Fig. 12 exhibits the spatial distribution of the anticipated risk of failure and the corresponding value of safety factor for cross section 6-6, for year 2006. Similar graphs were produced for all sections involved in the analysis. Furthermore, plots of stress distribution were produced and assessed. In Fig. 13 the distribution of Von Mises stress is presented corresponding to section 6-6 at the stage of first filling of the lake.

7. Comparisons and discussion

As already stated, the analysis was performed under plane-strain conditions. Therefore, in order to be able to compare the results of the FEM analyses with those obtained from the deformation monitoring, the vertical displacements observed at the control stations at the crest and the inspection gallery of the dam, were reduced to the cross section locations adopted in the FEM analysis. This was accomplished for every cross section in turn, by linear interpolation at the pairs of observed displacements,

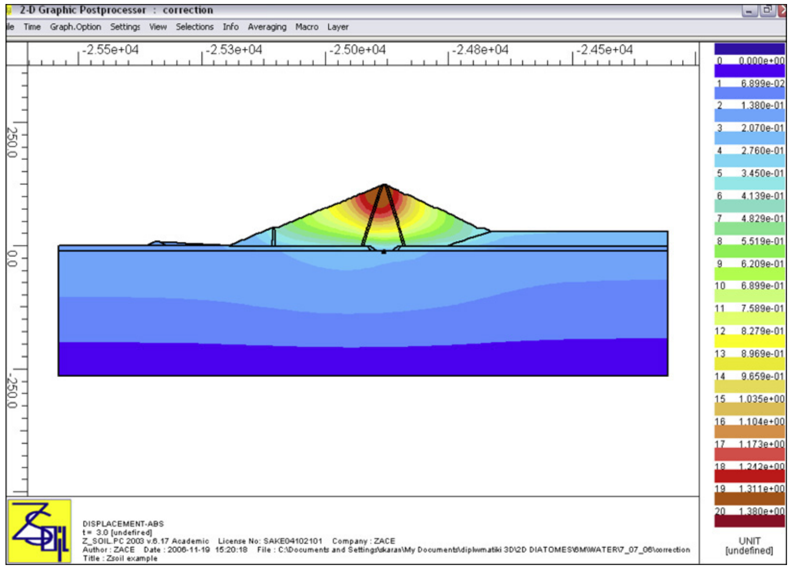

Fig. 11. Vertical displacements determined by finite element analysis at the central cross section 6-6 for the period 1973–1982.

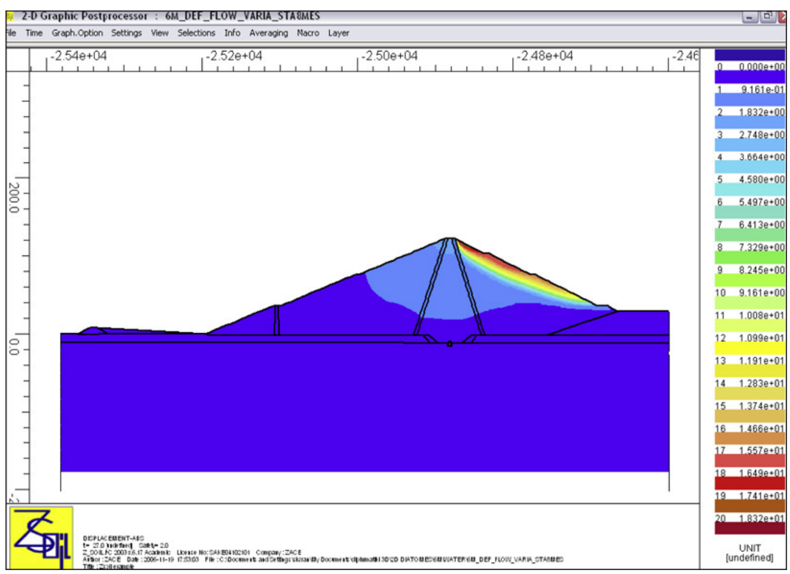

Fig. 12. Distribution of risk of failure at the central cross section 6-6 for year 2006; computed safety factor 1.9.

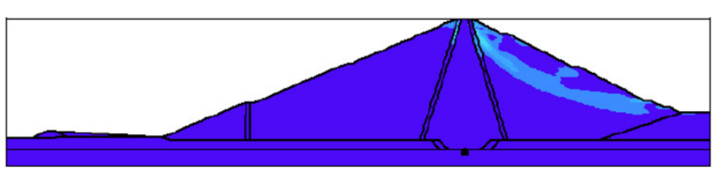

Fig. 13. Distribution of Von Mises stress for cross section 6-6 for year 2006 at the stage of first filling of the reservoir.

which correspond to the nearest control points from the FEM plane in question. Overall, comparisons were performed at the eleven cross section locations shown in Fig. 2.

In this paper, the authors show, merely as an example, a comparison obtained in a central cross section, where maximum displacements were observed. More specifically, Fig. 14 shows the cumulative vertical displacements estimated at section 6-6, based on three independent data sources, namely: precise leveling, magnetic extensometer and numerical modeling. The first thing to note from this diagram is a large systematic difference between the three estimates. This observation relates clearly to the differences in the time span of the available data. In fact, the precise leveling measurements start one year after the dam was completed and last until the present day, with only a small cut off in recent years. The magnetic extensometer settlements refer to the magnetic probe placed 3 m below the crest of the dam, and correspond to the period between the completion time of the dam until the sensor was disabled (1990). Finally, as discussed in the previous section, the FEM analysis results correspond to the main stages in the lifetime of the dam (Table 2).

Examination of Fig. 14 in more detail shows an apparent difference of the order of 0.65 m between the magnetic extensometer

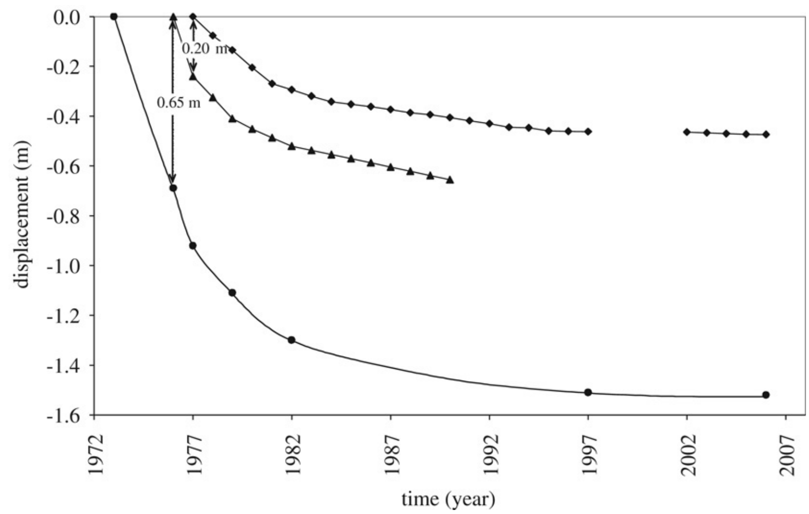

Fig. 14. Time series of vertical displacements determined at the dam crest, at cross section 6-6 by precise leveling (rhombs), magnetic extensometers (triangles) and FEM analysis (circles). The precise leveling data refer to station S20 and cover the period 1977–2006, the magnetic extensometer data refer to the magnetic sensor placed 3 m bellow the crest in 1976 and operated until 1990, and the FE computed displacements refer to specific times in the period 1973–2006.

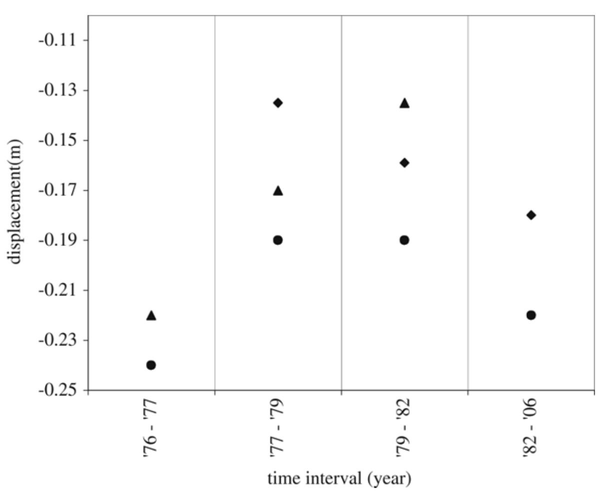

Fig. 15. Comparison of vertical displacements determined at the crest of the dam at cross section 6-6, for characteristic stages in the lifetime of the dam by precise leveling (rhombs), magnetic extensometers (triangles) and FEM analysis (circles).

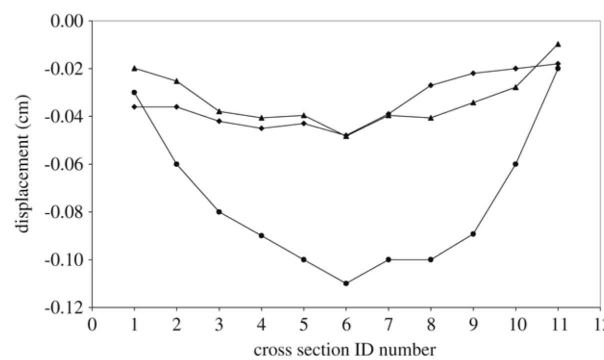

Fig. 16. Vertical displacements derived at the control stations at the gallery of the dam by precise leveling (rhombs) and FEM analysis (triangles) for the period 1977–2004, and by FEM analysis (circles) for the period 1973–2006.

measurements and the FEM estimates anticipated for year 1976. This is to be expected, as the dam body settles throughout the construction period (1973–1976). Similarly, the apparent difference of the order of 0.20 m, noticed between the magnetic extensometer measurements and the precise leveling for year 1977 is due to the total settlement that occurred in 1976 and during the first half of 1977. However, the most important thing to note from this diagram is that, on average, all three estimates exhibit very similar trends, suggesting that the field measurements as well as the FEM model and its implementation are correct. This general conclusion is further validated by examining the graph in Fig. 15. This graph shows the vertical displacements determined from the FEM analysis and the field measurements at certain stages in the lifetime of the dam, for the same location examined in Fig. 14. With only very limited examination of this plot, it is evident that the maximum difference does not exceed 0.06 m and the mean value is of the order of 0.03 m. Overall, these results add further confirmation that the field observations and the FEM model are correct.

As already outlined, in order to study the mechanical behaviour of the dam in a comprehensive manner, similar analyses to those undertaken at the crest of the dam were performed at the inspection gallery. Fig. 16 shows the vertical displacements predicted by the finite element model at the cross section locations adopted in the analysis for the entire lifetime of the dam (1973–2006), and for the period for which geodetic data are available (1977–2004). Also, in the same plot the geodetically derived vertical displacements are shown. Several conclusions can be drawn from this plot. Firstly, the maximum movement predicted by the FEM model for the period 1973–1976 is considerably smaller compared to the displacements determined at the crest of the dam for the same period (refer to Fig. 14), and in any case does not exceed 0.11 m. This is to be expected, as the settlement observed at the crest of the dam represents the accumulated compression over time of all underlying material. Also, the gallery was made of thick reinforced concrete which was adapted to withstand the gravity load and static water pressure. The second thing to note is that both the FEM predicted and geodetically derived displacements for the period 1977–2004, are small and vary up to 0.05 m. Moreover, it is important to note that they compare very well to each other and exhibit a mean difference better than 0.01 m.

8. Conclusions

The analysis of the deformation monitoring record of the Mornos dam revealed vertical displacements at the crest and the grouting gallery, with maximum movements occurring at the central cross sections of the dam. The vertical displacements of the dam are decreasing exponentially with time tending to their final values. The cross-comparison of the deformation analysis results with those obtained from the numerical analysis, proved that there is a good agreement between the field measurements and computed values. Experience from design and analyses of this project, shows that the combination of the FE method with deformation monitoring measures offers a feasible approach for verifying (or calibrating) the geometrical changes obtained from modeling studies, as well as for contributing to the physical interpretation of the underlying causes of these changes.

Acknowledgements

Acknowledgments are due to N. Tsoukas, Head of the Division of Major Works and to E. Peppes, Head of the Topographical Department of the Athens Water Supply Company for the helpful discussions and the suggestions during data analysis and evaluation. The FEM analysis was supported by the project Pythagoras. The projected is co-funded by the EU-European Social Fund and National resources – EPEAEK II.

References

[1] Sowers G, Sally H. Earth and rockfill dam engineering. London (UK): Asia Publishing House; 1962.
[2] ICOLD. Lessons from dam incidents. In: International commission of large dams. Abridged ed. MA (USA): USCOLD; 1973.
[3] Szostak-Chrzanowski A, Massièra M, Chrzanowski A, Hill CJ. Use of geodetic monitoring surveys in verifying design parameters of large earthen dams at the stage of filling the reservoir. In: 10th International symposium on deformation measurement. CA (USA): FIG; 2001.
[4] Szostak-Chrzanowski A, Massièra M, Chrzanowski A. Use of deformation monitoring results in solving geomechanical problems – case studies. Eng Geology 2006;79:3–12.
[5] Clough RW, Woodward RJ. Analysis of embankment stresses and deformations. J Soil Mech Found Div ASCE 1967;93(SM4):529–49.
[6] Finn WDL. Static and seismic behavior of an earth dam. Can Geotech J 1967; 4(1):28–37.
[7] Kulhawy FH, Duncan JM, Seed HB. Finite element analyses of stresses and movements in embankments during construction. Geotech. Eng. Report. Berkeley, CA, USA, (TE-69-4) 1969.
[8] US Army Corps of Engineers. Structural deformation surveying. Engineering Manual 1110-2-1009. Washington DC (USA); 2002.
[9] Wilson W. Deformation of earth and rockfill dams. In: Hirschfield RC, Poulos SJ, editors. Embankment dam engineering. Florida (FL, USA): Krieger Publishing Company; 1973.
[10] Pytharouli S, Stiros S. Ladon dam (Greece) deformation and reservoir fluctuations: Evidence for a causative relationship from the spectral analysis of a geodetic monitoring record. Eng Struct 2005;27:361–70.
[11] Szostak-Chrzanowski A, Massièra M, Chrzanowski A. Kinematic analysis of behavior of large earth dams. In: XXII FIG congress. Munich (Germany): FIG; 2006.
[12] Guler G, Kilic H, Hosbas G, Ozaydin K. Evaluation of the movements of the dam embankments by means of geodetic and geotechnical methods. J Surv Eng 2006;132(1):31–9.
[13] Lahmeyer International Consulting Engineers. Mornos dam: 780 million m^3 reservoir for water supply to Athens area. Technical report. Athens, Greece; 1976.
[14] Mitsakaki C, Stathas D. Reliability tests of Mornos dam control network. Scien J Technical Chamber of Greece 1983;3(1–4):57–79.
[15] Agatza-Balodimou A, Mitsakaki C. Deformation studies in the Mornos dam area. Surv Rev 1985;28:151–62.
[16] Gikas V, Paradissis D, Raptakis K, Antonatou O. Deformation studies of the dam of Mornos artificial lake via analysis of geodetic data. In: FIG Working Week. Cairo (Egypt): FIG; 2005.
[17] Avallone A, Briole P, Agatza-Balodimou AM, Billiris H, Charade O, Mitsakaki C, et al. Analysis of eleven years of deformation measured by GPS in the Corinth rift laboratory area. Geoscience Academie des Sciences, Paris 2004;336(4–5): 301–11.
[18] Billiris H, Paradissis D, Veis G, England P, Featherstone W, Parsons B, et al. Geodetic determination of tectonic deformation in central Greece from 1900 to 1988. Nature 1991;350:124–9.
[19] Balodimos DD. Development of a special trigonometric leveling technique. Scien J Technical Chamber of Greece 1979;3:31–8.
[20] Z_Soil. User manual. *Elmepress*, (www.zace.com). 2003.
[21] Agelopoulou O. Analysis of the Mornos dam with the finite element method – S-E section. Postgraduate research thesis. Geoinformatics interdisciplinary program of postgraduate studies. Athens (Greece): National Technical University of Athens; 2007.
[22] Karanasiou S. Analysis of the Mornos dam with the finite element method – N-W section. Postgraduate research thesis. Geoinformatics interdisciplinary program of postgraduate studies. Athens (Greece): National Technical University of Athens; 2007.
[23] Tsatsanifos C. Slope stability of the Mornos dam. M.Sc. thesis. London (UK): Imperial College; 1976.
[24] Wilson S, Hancock C. Instrumentation for movements within rockfill dams, STP41282S. ASCE; 1965.
[25] Drucker D, Prager W. Soil mechanics and plastic analysis or limit design. Q Appl Math 1952;10:157–65.

ID	Title	Pages
268780	Settlement analysis of the Mornos earth dam (Greece): Evidence from numerical modeling and geodetic monitoring	8